VI. ELECTRODYNAMICS OF MEDIA*

Academic Research Staff

Prof. W. P. Allis
Prof. C-I. Chang
Prof. L. J. Chu
Prof. H. A. Haus
Prof. P. W. Hoff
Prof. J. A. Kong
Prof. P. Penfield, Jr.

Graduate Students

E. L. Frohring
T. Holcomb
D. L. Lyon
A. H. M. Ross
E. E. Stark, Jr.
W. A. Stiehl
L. Tsang

A. ELECTRON DISTRIBUTION AND LASING EFFICIENCY OF DIATOMIC GAS LASER

The reported high efficiencies of the CO laser operating in the 5μ range have made this laser of particular interest as a potential high-efficiency source of infrared radiation. Computer studies by Nighan[1] have determined the electron distribution in the commonly employed laser mixture of He and CO. In Nighan's studies, all gas atoms were assumed to be in the ground state. Later work by the same author[2] showed that the electron distribution is not greatly modified if the presence of lasing atoms in higher lying states is taken into account. Novgorodov et al.[3] have shown good agreement with Nighan's computations for CO_2-N_2. Lacina[4] has made computations of the population distribution over the vibrational levels of the CO lasing molecule. Similar studies have been made by A. W. Ross.[5] These distributions were determined for given electron distributions and did not take into account the reaction of the molecular population distribution on the electrons.

When attempting to predict saturation parameters and lasing efficiencies in a reliable way, it is necessary to solve self-consistently the problems of electron distribution and of lasing molecules over the vibrational levels. Such studies will doubtless be completed in the near future, but even when the results are available, it will still be of interest to have a model of a diatomic gas laser which permits closed-form solutions.

In this report we present a model of a diatomic laser gas that has the level structure of a harmonic oscillator, and exchanges energy via vibrational-translational collisions with a background gas. The electrons pumping the lasing molecules are described by a distribution function in velocity space obeying a differential equation that can be solved in closed form under certain simplifying assumptions. The excitation

*This work was supported by the Joint Services Electronics Programs (U.S. Army, U.S. Navy, and U.S. Air Force) under Contract DAAB07-71-C-0300, and by U.S. Air Force Cambridge Research Laboratories Contract F19628-70-C-0064.

of the diatomic molecules is related to the electron distribution. We determine a limit on the efficiency of conversion between electrical energy and optical energy.

1. Electron Gas

Electrons driven by a field E through a gas background tend to maintain a spherically symmetric velocity distribution as long as the electric field is not excessive. This is the case for the values of E/N (where N is the number density of the gas) employed in gas laser discharges. We describe the electron distribution by the function f(v), where v is the radial coordinate in velocity space in a spherical coordinate system. The distribution function is normalized.

$$\int 4\pi v^2 f(v)\, dv = 1. \tag{1}$$

In the steady state, electrons are put in and taken out of a particular velocity range v, v+dv by the driving electric field, by the elastic collisions, and by energy transfer from the gas atoms at temperature T_g. These contributions are listed in order.[6]

$$4\pi v^2 dv \left.\frac{\partial f(v)}{\partial t}\right|_{e\ell} = -4\pi \frac{\partial}{\partial v}\left\{\frac{v^2}{3}\frac{\left(\frac{e}{m}E\right)^2}{\nu_m}\frac{\partial f}{\partial v} + \eta v^3 \nu_m\left(f + \frac{kT_g}{mv}\frac{\partial f}{\partial v}\right)\right\} dv, \tag{2}$$

where $\eta = m/M+m$, with m the electron mass and M the mass of the molecule, and ν_m is the frequency of momentum-transfer collisions.

It is convenient to use as an independent variable the energy in electron volts,

$$u \equiv \frac{mv^2}{2e}. \tag{3}$$

Furthermore, it is also convenient to introduce a function $G_{e\ell}$, whose differential, $dG_{e\ell}$, gives the rate of exit of electrons from a particular energy interval, du, by the processes described above:

$$dG_{e\ell} = \frac{\partial G_{e\ell}}{\partial u} du = -4\pi d\left\{\frac{v^2}{3}\frac{\left(\frac{e}{m}E\right)^2}{\nu_m}\frac{\partial f}{\partial v} + \eta v^3 \nu_m\left(f + \frac{kT_g}{mv}\frac{\partial f}{\partial v}\right)\right\}$$

$$= -4\pi d\left\{\sqrt{\frac{2e}{m}}\,2\,\frac{\left(\frac{e}{m}E\right)^2}{3\nu_m}u^{3/2}\frac{\partial f}{\partial u} + \eta\left(\frac{2e}{m}\right)^{3/2}\nu_m u^{3/2}\left(f + \frac{kT_g}{e}\frac{\partial f}{\partial u}\right)\right\}. \tag{4}$$

The G-function has a simple interpretation of electron "current" in one-dimensional energy space. Indeed, if we define a current in energy space C, it has to obey the continuity law in the steady state.

$$\frac{\partial C}{\partial u} = -\text{ rate of particle entry/unit energy}$$

$$= +\text{ rate of particle exit/unit energy} = \frac{\partial G}{\partial u}.$$

By integration, and noting that G = 0 at u = 0, by definition, we get C = G.

Next, consider the process of electronic excitation. Suppose that electrons excite electronic levels of the atoms and/or molecules when they possess a sharply defined energy u_x. Then electrons are being taken out of the energy range u_x, $u_x + du$ and returned with essentially zero energy at u = 0. A G-function, G_x, may be defined for this process, whose derivative gives the rate of exit of electrons arising from the electronic excitation process,

$$\frac{\partial G_x}{\partial u}\, du = \nu_x \delta(u-u_x)\, du - \nu_x \delta(u)\, du. \tag{5}$$

Here, ν_x is the electronic excitation frequency, and δ is the Dirac delta function.

In CO, the excitation of vibrational levels by the electrons occurs through the formation of a negative ion state. The excitation of the state requires 1.8 eV energy. Upon excitation, the electrons lose an energy $h\nu_v$, where $h\nu_v$ is the vibrational energy interval, if the excitation carries the molecule from the 0 state to the 1 state. The energy loss is approximately $2h\nu_v$ if the molecule is excited from the 0 to the 2 state, and so forth. We shall make the approximation that all electrons lose an energy Δu upon an exciting collision with a CO molecule, when they reach an energy $u_e + \Delta u$, where $u_e \approx 1.8$ eV. We shall assume that Δu, which in general is greater than $h\nu_v/e$, is small enough when evaluating the differential equation for the distribution function. The derivative of the G-function associated with molecular excitation,

$$\frac{\partial G_e}{\partial u}\, du = \nu_e \delta(u-u_e-\Delta u) - \nu_e \delta(u-u_e),$$

may be approximated by a "doublet," a derivative of a delta function ($\nu_e \to \infty$, $\Delta u \to 0$).

This approximation greatly simplifies the mathematics. Note in particular that the energy loss by electrons in the energy range $u_1 < u < u_2$ is given by

$$\int_{u_1}^{u_2} u\, \frac{\partial G_e}{\partial u}\, du = uG_e\Big|_{u_1}^{u_2} - \int_{u_1}^{u_2} G_e\, du. \tag{6}$$

If the derivative of G_e is a doublet, then G_e itself is a delta function, and the content of the delta function is equal to the rate of energy loss by the electrons. If the electron collision frequency is ν_e, then

$$-\int G_e \, du = \Delta u \nu_e. \tag{7}$$

By setting the sum of $G_{e\ell}$, G_x, and G_e equal to zero, we obtain a differential equation for f(u). We make the further approximation that the elastic losses and the energy exchange with the gas at temperature T_g are negligible. We set $\nu_m = vQ_mN$. We assume that the collision cross section for momentum exchange, Q_m, is inversely proportional to the velocity because this leads to a simple final expression, and write

$$Q_m = Q\sqrt{\frac{u_o}{u}}. \tag{8}$$

The result is

$$f(u) = 2K\left\{\frac{1}{\sqrt{u}} - \frac{1}{\sqrt{u_x}}\right\}\frac{\nu_x}{N}\left(\frac{N}{E}\right)^2; \quad u_e + \Delta u < u < u_x$$

$$= 2K\left\{\frac{1}{\sqrt{u}} - \frac{1}{\sqrt{u_x}} + \frac{\nu_e}{\nu_x}\frac{\Delta u}{2u_e^{3/2}}\right\}\frac{N\nu_x}{E^2}; \quad 0 < u < u_e, \tag{9}$$

where we have defined the quantity

$$K \equiv \frac{3}{2\pi}\left(\frac{m}{2e}\right)^2 Q\sqrt{u_o}, \tag{10}$$

which is a constant for any specific system.

Utilizing the normalization condition (1) gives

$$L\left[\left(\frac{\nu_x}{N}\right) + \frac{\Delta u}{u_x}\left(\frac{\nu_e}{N}\right)\right] = \left(\frac{E}{N}\right)^2, \tag{11}$$

where

$$L = \frac{4\pi}{3}K\frac{u_x}{\left(\frac{m}{2e}\right)^{3/2}} = 2\left(\frac{m}{2e}\right)^{1/2} Q\sqrt{u_o}\, u_x, \tag{12}$$

which depends on the electronic excitation energy u_x.

2. Excitation of Diatomic Molecules

We assume that the lasing molecular species can be described by a diatomic, harmonic oscillator model. The Landau and Teller[7, 8] model gives the coefficients of the rate equation as functions of energy level for vibrational-translational (V-T) collisions and for vibrational-vibrational (V-V) collisions. These[8] are introduced as follows.

$$\frac{dx_n}{dt} = ZP_{10}\left\{(n+1)x_{n+1} - \left[(n+1)e^{-\theta_g} + n\right]x_n + ne^{-\theta_g}x_{n-1}\right\}$$

$$+ ZQ_{10}N_M\{(n+1)(1+\alpha_v)x_{n+1} - [(n+1)\alpha_v + n(1+\alpha_v)]x_n + n\alpha_v x_{n-1}\}$$

$$+ n_e P_e\{(n+1)x_{n+1}f(u_e) - [(n+1)f(u_e+\Delta u) + nf(u_e)]x_n + nf(u_e+\Delta u)x_{n-1}\}$$

$$- R(\delta_{n,\ell+1} - \delta_{n,\ell}). \qquad (13)$$

Here, x_n is the fractional occupation of the n^{th} vibrational level of the diatomic molecule; ZP_{10} gives the rate of V-T relaxation; θ_g is related to the gas temperature T_g by

$$\theta_g = \frac{h\nu_v}{kT_g}, \qquad (14)$$

where $h\nu_v$ is the energy separation of the vibrational levels; $ZQ_{10}N_M$ gives the rate of V-V relaxation, with N_M the number density of "active" molecules; and α_v is a measure of the energy in vibrational levels

$$\alpha_v \equiv \sum_0^\infty nx_n.$$

The term in the third row of Eq. 13 gives the excitation by the electrons in terms of an excitation "cross section" P_e. The excitation "cross section" depends on the energy level, and we assume that the cross sections are also given by the Landau-Teller model. This is a reasonable assumption because the interaction potentials of the molecule with the electron are dipole potentials. The last term in Eq. 13 gives the rate of transition caused by the laser radiation. We assume that the radiation operates between the upper level $\ell+1$ and the lower level ℓ. This rate is proportional to the laser intensity I, but also involves the actual populations of the levels

$$R = \beta IN_M(x_{\ell+1} - x_\ell)\exp\{-B[(J_\ell+1)J_\ell - (J_{\ell+1}+1)J_{\ell+1}]/kT_g\}, \qquad (15)$$

where β is a proportionality constant which depends, among other things, on the matrix element squared of the transition, and B is the rotational constant.

An equation for the energy parameter α_v in Eq. 13 may be obtained from it by a simple manipulation. We multiply the set of equations each by n and sum. When the summations are evaluated, the result is

$$\nu_e^M - \frac{\alpha_v - \alpha_g}{\tau_g} - R = 0, \tag{16}$$

where we have defined the relaxation rates

$$\frac{1}{\tau_g} \equiv ZP_{10}\left(1 - e^{-\theta_g}\right); \quad \nu_e^M = n_e P_e\{(1+\alpha_v)f(u_e+\Delta u) - \alpha_v f(u_e)\}, \tag{17}$$

and α_g is defined analogously to α_v.

In general, knowledge of α_v is not sufficient to know the distribution of particles over the vibrational levels. In the limit, however, when the V-V rates become very fast, the second term in parenthesis in Eq. 13 must vanish. This must be so if the product of $ZQ_{10}N_M$ times the term in braces is to remain finite as $ZQ_{10}N_M$ goes to infinity. As a consequence, the distribution over vibrational levels must be Boltzmann-like at the temperature characterized by α_v and related to α_v by

$$\frac{\alpha_v}{1 + \alpha_v} = \exp(-h\nu_v/kT_v). \tag{18}$$

Equation 16 then incorporates everything we need to know about the effect of the electrons and the laser field upon the vibrational system.

We have introduced two vibrational excitation rates, ν_e and ν_e^M. The latter gives the rate of electron excitations, the former the rate of molecular excitations. The number of electron collisions per unit volume is $\nu_e n_e$, which must be equal to the number of exciting collisions of the molecular species of density N_M.

$$\nu_e^M = \frac{n_e}{N}\left(\frac{N}{N_M}\right)\nu_e = \frac{n_e}{N}\,\frac{\nu_e}{C_M}, \tag{19}$$

where $C_M \equiv N_M/N$. Now ν_e itself depends upon the operating conditions. This dependence is discussed below.

From (16) it is clear that the rate of energy supply to the lasering gas by the electrons is

$$n_e \nu_e \Delta u = N_M \nu_e^M \Delta u$$

$$= \Delta u n_e P_e N_M \{(1+\alpha_v) f(u_e+\Delta u) - \alpha_v f(u_e)\}. \tag{20}$$

Now, from Eqs. 9 and 11, we obtain $f(u_e)$ and $f(u_e+\Delta u)$ for given $\nu_e \Delta u$. By introducing this into Eq. 20, we get

$$\frac{n_e}{NC_M}\nu_e = n_e P_e 2K\left(\frac{N}{E}\right)^2 \frac{\nu_x}{N}\left\{\frac{1}{\sqrt{u_e}} - \frac{1}{\sqrt{u_x}}\right\}$$

$$\cdot \left\{(1+\alpha_v) - \alpha_v\left[1 + \frac{(\nu_e+\nu_x)}{\nu_x}\,\frac{\Delta u}{2u_e\left(1-\sqrt{\frac{u_e}{u_x}}\right)}\right]\right\}. \tag{21}$$

We solve for ν_e and get

$$\nu_e = \nu_x \frac{T(1-\alpha_v S)}{\left(\frac{E}{N}\right)^2 + TS\alpha_v}, \tag{22}$$

where

$$T = 2P_x C_M K\left\{\frac{1}{\sqrt{u_e}} - \frac{1}{\sqrt{u_x}}\right\} \tag{23}$$

and

$$S = \frac{\Delta u}{2u_x\left(1-\sqrt{\frac{u_e}{u_x}}\right)}. \tag{24}$$

Note that, for given E/N, ν_e decreases with increasing α_v when the vibrational temperature increases. This is so because the rate of down-transitions produced by the electrons increases as α_v increases, for a given discontinuity in f(u); (cf. Eq. 17). Furthermore, we note that ν_e decreases with increasing $(E/N)^2$; the largest value of ν_e is reached for fixed α_v when E/N = 0. This is clearly wrong, and occurs because of our assumption that elastic losses are negligible. There should be enough of an E-field to overcome the losses, so that a sufficient number of electrons is brought to the energy u_e to excite the lasering species. Only when this field has been reached will a further increase of the field lead to a decrease of ν_e. Thus, for Eq. 22 to be valid,

$(E/N)^2 > (E_c/N)^2$, where E_c is this critical field. For the evaluation of E_c, we need an analysis that takes into account the elastic loss.

3. Comparison with Nighan's Results

Nighan[1] has presented detailed computations for the electron distribution in CO. We want to study how the analysis presented here meshes with Nighan's results. In order to make approximations equivalent to his, we assume that all molecules are in the ground state, $a_v = 0$. It is then possible to find ν_x and ν_e in terms of E/N, by using Eqs. 22 and 11, which results in

$$\nu_x = \frac{(E/N)^4}{\frac{L}{N}\left[\left(\frac{E}{N}\right)^2 + T\frac{\Delta u}{u_x}\right]} \tag{25}$$

$$\nu_e = \frac{T\left(\frac{E}{N}\right)^2}{\frac{L}{N}\left[\left(\frac{E}{N}\right)^2 + T\frac{\Delta u}{u_x}\right]}. \tag{26}$$

The parameter T is defined by (23) and may be interpreted from Eqs. 25 and 26 in terms of ν_e, in the limit of large E/N.

$$T = \nu_e\Big|_{E\to\infty}\frac{N}{L} = \frac{m}{e}\frac{u_x}{N^2}\nu_m\nu_e\Big|_{E\to\infty}. \tag{27}$$

The excitation rate ν_e at large field intensity is a function of the parameter P_e in (13). Alternatively, we may use Nighan's[1] Figure 12 to read off

$$\nu_e\Big|_{E\to\infty} \cong 2\times 10^{-8}\times N. \tag{28}$$

We may use this one result to find all other dependences. Thus, for example, the fractional power transfers

$$\frac{\nu_e\Delta u}{\nu_x u_x + \nu_e\Delta u} \quad \text{and} \quad \frac{\nu_x u_x}{\nu_x u_x + \nu_e\Delta u} \tag{29}$$

behave qualitatively like those shown in Nighan's[1] Figure 8. The two are equal at a field intensity given by

$$\frac{E}{N} = \sqrt{T \frac{\Delta u}{u_x}}. \tag{30}$$

Using the value of T obtained previously, we have

$$\frac{E}{N} = \sqrt{\frac{m}{e} \frac{\nu_m}{N} \frac{\nu_e}{N} \Delta u} = 0.6 \times 10^{-15} \tag{31}$$

for the crossover between the two rates of (29), $\nu_m/N = 10^{-7}$ and $\Delta u = 0.2$ eV. This compares reasonably well with Nighan's[1] Figure 8.

Next, consider the plot of ν_e vs $\bar{u}_r$ as defined by Nighan. It is an easy matter to check that the function f(u) has the two limiting forms for small and large E as shown in Fig. VI-1. We find

$$\lim_{E \to 0} \bar{u}_r = \frac{2}{3} \int u^{2/3} f(u)\, du \Big|_{E \to 0} = \frac{2}{5} u_e \tag{32}$$

and

$$\lim_{E \to \infty} \bar{u}_r = \frac{u_x}{5}.$$

Now, for $u_e = 1.8$ eV and $u_x \approx 14$ eV, $\bar{u}_r$ ranges from 0.7 eV to 2.8 eV. The value of u_x is somewhat uncertain and must be adjusted so that reasonable results are obtained.

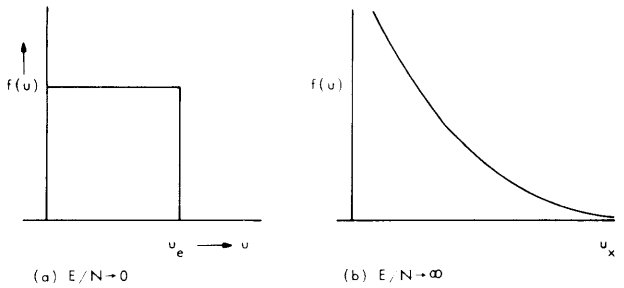

Fig. V-1.
Limiting form for f(u).

In CO, the ionization energy is 14 eV; the first excitation is at 6 eV. If we set u_x too low in the simple model presented here, then the electron energy $\bar{u}_r$ "saturates" at too low a value.

4. Upper Limit on Efficiency

One way of realizing that the efficiency cannot exceed unity (i.e., a heat-operated laser is impossible) is to note from (16) that

$$NC_M R = n_e \nu_e - \frac{\alpha_v - \alpha_g}{\tau_g} NC_M, \tag{33}$$

and that α_v must exceed α_g if gain is to be attained. Indeed, from Eq. 15 we find that, for gain to exist, we need

$$\frac{\alpha_v}{1+\alpha_v} > \exp\left[\frac{-2B(J_\ell+1)}{kT_g}\right] = \left[\frac{\alpha_g}{1+\alpha_g}\right]^{[2B(J_\ell+1)]/h\nu_v} \tag{34}$$

Now, $2B(J_\ell+1)/h\nu_v \ll 1$, and $\alpha_g/(1+\alpha_g) \approx \alpha_g \ll 1$, which results approximately in

$$\alpha_v > \frac{h\nu_v}{2B(J_\ell+1)\ \ln\frac{1}{\alpha_g}} \approx \frac{kT_g}{2B(J_\ell+1)}. \tag{35}$$

For a given rotational transition and gas temperature, α_v has a lower limit below which laser gain ceases:

$$\alpha_{v_{min}} = kT_g/2B(J_\ell+1). \tag{36}$$

An upper limit on the efficiency may be obtained by disregarding the heating of the gas [the term $(\alpha_v-\alpha_g)/T_g$ in (33)]. Then all of the power transferred to vibration is assumed to appear as useful laser power. The efficiency η is thus limited by

$$\eta \leq \frac{\nu_e \Delta u}{\nu_x u_x + \nu_e \Delta u}. \tag{37}$$

Now, ν_e is to be made as large as possible, ν_x as small as possible. This is achieved at low E/N. From (22),

$$\nu_{e_{max}} \leq \frac{\nu_x}{\alpha_{v_{min}} S}\left(1 - \alpha_{v_{min}} S\right). \tag{38}$$

Introducing this expression into (37), we have

$$\eta \leq \frac{1}{1 + \frac{u_x}{\Delta u}\alpha_{v_{min}} S} \approx \frac{1}{1 + \frac{u_x}{2u_e}\alpha_{v_{min}}}. \tag{39}$$

For CO, for which the rotational frequency separation is of the order of 100 GHz,

$\alpha_{v_{min}}$ evaluates to approximately unity. The efficiency is then

$$\eta \leq \frac{1}{1 + \frac{u_x}{2u_e}}. \tag{40}$$

Introducing $u_x = 6$ eV, we have $\eta \leq 40\%$. A larger value of u_x gives smaller efficiencies. A possibility for obtaining larger efficiencies stems from the fact that anharmonicity of the CO molecules causes a non-Boltzmann distribution with much higher effective temperatures for higher vibrational levels. The curves of Center and Caledonia[10] suggest that $\alpha_v \approx 0.27$ for the lower vibrational levels permits an effective $\alpha_{v|\,eff} \approx 8$ for the lasing levels. Much higher efficiencies could then be predicted from (40).

The main conclusion from the study of efficiency is that electronic excitations put a severe limitation on the efficiency. Operation at low E/N is desirable to reduce them. Furthermore, the Treanor-Rich[11] distribution of the higher lying vibrational levels permits operation of the laser at relatively low vibrational temperatures of the lower vibrational levels, and hence at beneficially low E/N values, provided the discharge is maintainable at such E/N values.

5. Extension to Study of Discharge Characteristics

The present formalism can be extended to study gas laser discharges. It may be assumed that the rate of ionization ν_i is some fraction κ of the rate of electronic excitation,

$$\nu_i = \kappa \nu_x. \tag{41}$$

The ionization frequency itself is determined by diffusion and recombination losses

$$\nu_i = a n_e + D/\Lambda^2. \tag{42}$$

We repeat the other pertinent equations.

Normalization Conditions

$$L\left[\left(\frac{\nu_x}{N}\right) + \frac{\Delta u}{u_x}\left(\frac{\nu_e}{N}\right)\right] = \left(\frac{E}{N}\right)^2 \tag{43}$$

Energy Balance for Vibrational Excitation

$$\frac{n_e}{NC_M}\nu_e - \frac{\alpha_v - \alpha_g}{\tau_g} - R = 0 \tag{44}$$

Law of Energy Conservation

$$\frac{JE}{e} = n_e(\nu_x u_x + \nu_e \Delta u + \nu_i u_i) \tag{45}$$

Finally, the equation for ν_e in terms of E/N is

$$\nu_e = \nu_x \frac{T(1-\alpha_v S)}{\left(\frac{E}{N}\right)^2 + TS\alpha_v}. \tag{46}$$

For any given E and laser radiation R, we have six equations for the six unknowns: ν_i, ν_x, ν_e, n_e, J, and α_v. This set of equations is sufficient to find V-I characteristics and other physical information.

W. P. Allis, H. A. Haus

References

1. W. L. Nighan, Phys. Rev. A 2, 1989-2000 (1970).
2. W. L. Nighan, Private communication.
3. M. Z. Novgorodov, A. G. Srizidov, and N. N. Sobolev, IEEE J. Quant. Electronics, Vol. QE-7, pp. 508-511, November 1971.
4. W. B. Lacina, NCL 71-32R, Northrop Corporate Laboratories.
5. A. W. Ross, Unpublished work.
6. W. P. Allis, "Motions of Ions and Electrons," in S. Flügge (Ed.), Handbuch der Physik, Vol. 21 (Springer Verlag, Berlin, 1956), pp. 383-444; also Technical Report 299, Research Laboratory of Electronics, M.I.T., June 13, 1956.
7. L. Landau and E. Teller, Physik. Z. Sowjetunion 10, 34-41 (1936).
8. A. I. Osipov and E. V. Stupochenko, Soviet Phys. – Usp. 6, 47-63 (1963) (translation); or Usp. Fiz. Nauk 79, 81-113 (1963).
9. R. D. Hake and A. V. Phelps, Phys. Rev. 158, 70 (1967).
10. R. E. Center and G. E. Caledonia, Appl. Opt. 10, 1795-1802 (1971).
11. C. E. Treanor, J. W. Rich, and R. G. Rehm, J. Chem. Phys. 48, 1798 (1968).

B. MEASUREMENT OF THE V-V RELAXATION RATE IN THE ASYMMETRIC STRETCH MODE OF CO_2

We have measured the V-V relaxation rate of the asymmetric stretch mode of CO_2, that is, the rate at which the occupancies of states $\nu_3 = 0, 1, 2, \ldots$ relax toward a Boltzmann equilibrium at some vibrational temperature T_3. Most other rates of interest in the CO_2 laser system are well known, but this rate has not been measured previously. In part this is because the strong radiation trapping of the 4.3 μ fluorescence band makes

it impossible to monitor spectroscopically the populations of individual levels in the asymmetric stretch mode.[1]

This study was made in a TEA CO_2 amplifier, using unusual pulse amplification results. Under normal circumstances, we could expect three types of amplifier results. At very low pressures, with short, intense pulses, coherent amplification effects[2] such as nutation can occur. Under these conditions, the population in only a single rotational level can contribute to the amplification. In this regime, pulses of lower power will undergo bandwidth-limited amplification.

For longer pulses at higher pressures, saturated amplification may occur. For pulses that are long compared with T_2 all rotational levels in the 001 vibrational level can contribute, and lead to zero gain as the 001 and 100 populations equalize.

Finally, for pulses that are very long compared with the pumping time of the upper laser level by N_2, the gain will saturate at some positive level.

We have performed amplification experiments with pulses much longer than T_2 but much shorter than the pumping time of the upper laser level by N_2. The pulses were produced by cavity-dumping a CO_2 TEA laser. Typically, the cavity contained one long self-mode-locked pulse, which was "dumped" inefficiently; that is, it leaked out on two different round trips in the cavity, and thus led to a double-peaked pulse. The experimental system is shown in Fig. VI-2.

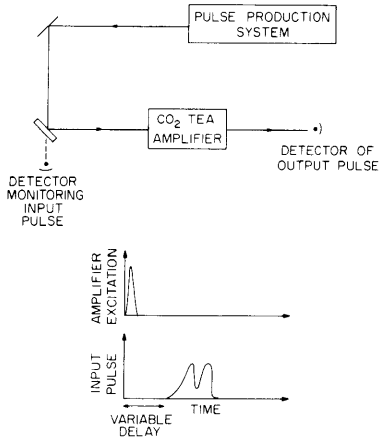

Fig. VI-2.

Experimental system for passing a laser pulse through an amplifier, with variable delay between the amplifier excitation and arrival of the pulse.

Timing circuitry permitted an adjustable delay between the current pulse in the amplifier and the arrival of the laser pulse for amplification. For this experiment, pressures in the range 50-200 Torr were used, with a 17.5 kV excitation voltage.

Figure VI-3 shows a typical result at 75 Torr pressure, with gas ratios $He:CO_2:N_2$ 12:3:1, and a 6-μs delay. Surprisingly, the second peak of the pulse is amplified more than the first peak. This was observed with and without N_2 in the amplifier,

for delays up to 8 μs and pressures up to 100 Torr. In this regime, the available vibrational population inversion should be depleted by the first part of the pulse, because of fast rotational relaxation. When N_2 is present, there is no opportunity for it to pump

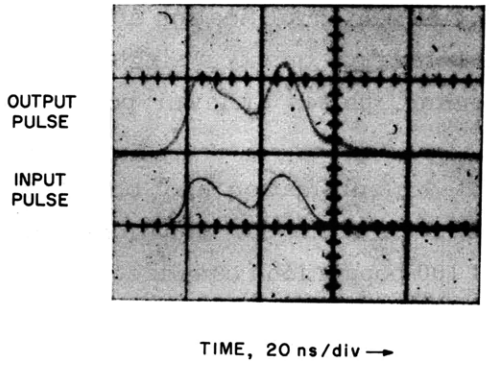

Fig. VI-3.

Typical experimental results. Peak power, 100 kW. Note that the second peak experiences higher gain than the first.

the 001 level measurably within 20 ns, and at best the lower level can be depleted somewhat by relaxation into the $\nu_2 = 2$ level of the bending mode. Thus we would expect to see, at best, a reduced gain at the second peak. The only explanation for our observations is that, between the two peaks, the asymmetric mode has relaxed toward a Boltzmann equilibrium at a new, lower vibrational temperature, and hence 001 has been repopulated. The increase in gain could be observed only if the asymmetric mode were so hot in the beginning that a decrease in T_3 would lead to an increase in the population of 001. In the present system, this can occur only at low amplifier pressures, at which the discharge excites the vibrational modes heavily. This can be understood from Fig. VI-4.

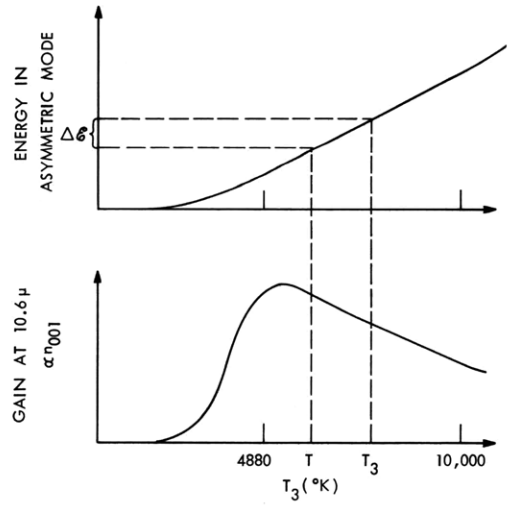

Fig. VI-4. Illustration of how the extraction of energy from the asymmetric mode causes a decrease in the equilibrium temperature of that mode, and hence an increase in gain.

If T_3 begins above 4880°K and an energy $\Delta \mathscr{E}$ is extracted from the chain during the first peak of the pulse, the asymmetric mode will relax toward a Boltzmann equilibrium at a new temperature T^*. At this temperature, the population in 001 will be larger than before, and hence there can be a higher gain in the latter parts of an amplified pulse. For these pulses and pressures, the interval between the two peaks contains roughly five CO_2-CO_2 intercollision times. The dominant process will be 002 + 000 → 001 + 001. Our observation of enhanced gain indicates that the probability that this reaction will occur in a collision will be ~0.2.

For delays longer than 8 μs, and for pressures above 100 Torr, normal gain saturation was observed; that is, there was reduced gain on the second peak of the pulse. Above 100 Torr, the asymmetric chain cannot be pumped sufficiently hot to allow us to observe this effect. When there is a long delay between the amplifier excitation and the pulse arrival, the asymmetric chain has relaxed below 4880°K by interaction with the symmetric chain, so that only gain saturation can be observed.

This effect is of great importance in the design of high-power CO_2 amplifier systems. Pumping the asymmetric chain to a higher temperature does yield higher stored energy, which is available if a pulse is long enough to take advantage of this V-V relaxation process. Also, this increased storage is not accompanied by a corresponding increase in small-signal gain, especially for large T_3, so that the problem of superradiance is not increased.

E. E. Stark, Jr., P. W. Hoff

References

1. L. O. Hocker, M. A. Kovacs, C. K. Rhodes, G. W. Flynn, and A. Javan, Phys. Rev. Letters 17, 233 (1966).
2. P. W. Hoff, H. A. Haus, and T. J. Bridges, Phys. Rev. Letters 25, 82 (1970).
3. E. E. Stark, Jr., and P. W. Hoff, Quarterly Progress Report No. 105, Research Laboratory of Electronics, M.I.T., April 15, 1972, pp. 77-79.

C. MEASUREMENT OF THE SPECTRUM OF A TEA CO_2 LASER

In 1970, Beaulieu reported the observation of laser action at 10.6 μm in a CO_2-N_2-He mixture at pressures as high as atmospheric.[1] The new transversely excited atmospheric (TEA) pressure CO_2 laser can generate much higher average powers per unit volume than conventional low-pressure CO_2 lasers, and gives promise of being a tunable, wideband pulsed source in the infrared. Recently efforts have been made[2,3] to determine the spectrum of the TEA CO_2 laser by using a scanning Fabry-Perot interferometer, but the results have been limited by the resolution of the instrument, and they are not based on a single shot. We are reporting what we believe to be the first measurements of the

dynamic frequency of individual TEA laser pulses.

1. Experimental Arrangement

The optical heterodyne experiment is illustrated in Fig. VI-5. The TEM_{00} modes from a single-longitudinal-mode TEA laser and a stable cw CO_2 laser are aligned and focused onto a Ge:Cu(Sb) detector, D1, which is cooled to 4.2°K. The difference in optical frequencies is observed on a high-speed oscilloscope as a beat signal superimposed on the envelope of the TEA pulse. When the beat frequency is found to be stable from pulse to pulse, a spectrum analyzer is used to display the spectral distribution of a series of pulses.

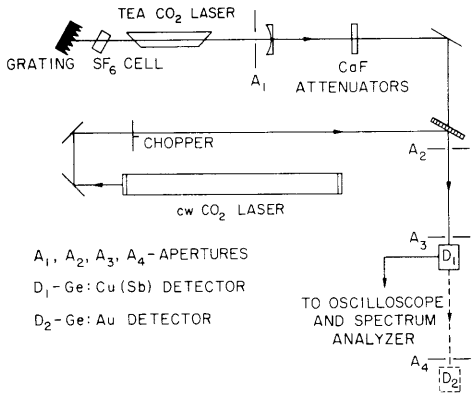

Fig. VI-5.
Experimental arrangement.

The TEA cavity is defined by a 72-line/mm aluminum diffraction grating for selection of the P(20) transition in CO_2 separated 75 cm from a curved 80% reflecting germanium mirror of 4-m curvature radius. The SF_6 cell is for longitudinal-mode selection. Aperture A1 is for transverse-mode selection. The electrodes comprise the leads of sixty-one 1-kΩ carbon resistors as anodes, with an equal number of pins for cathodes, 1 in. apart and diametrically opposed, in the helical distribution used by Beaulieu.[4] The electrode assembly is 12 in. long with a pitch of 6.5 in. The tube is sealed with NaCl flats at the Brewster angle. A gas mixture at 330 Torr containing 13% CO_2, 6% N_2, and 81% He is replaced 10 times per minute. A low-inductance 0.025 μF capacitor, charged to 17 kV, is discharged through the pins via a triggerable spark gap at 2 pulses/second. The laser pulse rise time is ~75 ns, and the half-power full width is 130 ns, which is typical of the TEA CO_2 laser.

The 5 W cw CO_2 laser is sealed and water-cooled. A CO_2-N_2-H_2-He mixture at 11 Torr is maintained in a 12-mA current discharge. The bore diameter is 0.5 in. The mechanical construction ensures good thermal stability. The laser operates on the P(20) transition at 10.6 μm.

Both beams pass through the centers of apertures A2 and A4, which are 320 cm apart;

the optical paths must be collinear within a milliradian. The nitrogen-cooled Ge:Au detector, D2, is used for alignment. No effort was made to mode-match the beams, and aperture A3, of 2-mm diameter, was required for spatial filtering of the combined beam. Detector D1 and the Tektronix 7904 oscilloscope both have bandwidths greater than 500 MHz.

2. Results

With the SF_6 for frequency-selective absorption and the high loss introduced by aperturing, only one longitudinal mode (occasionally two modes, 200 MHz apart) will oscillate near the center of the collision-broadened, 1600 MHz wide, gain curve of the TEA laser. The cw (reference) laser oscillates within approximately 10 MHz of line center ν_o.

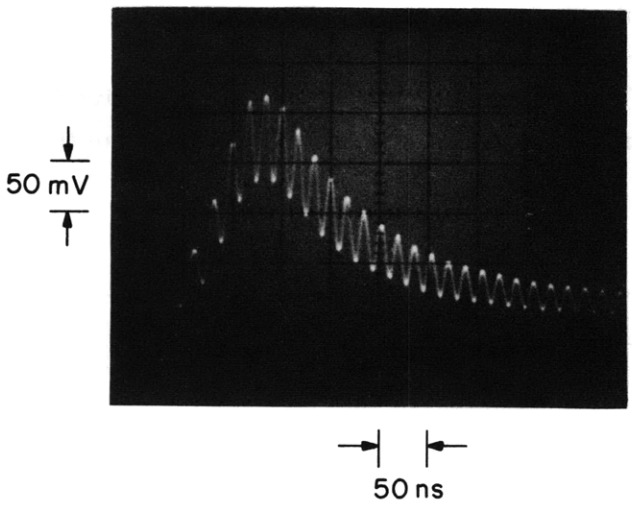

Fig. VI-6.

Time-resolved beat signal. Beat frequency 60 MHz.

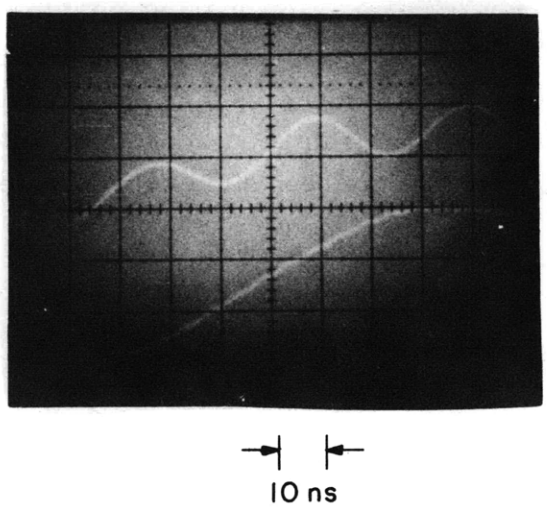

Fig. VI-7.

Detector output during a part of a pulse. Beat frequency 32 MHz. Upper: without the stable laser blocked. Lower: with the stable laser blocked.

Figure VI-6 shows a time-resolved beat signal, which indicates that the TEA frequency is 60 MHz from the reference frequency near ν_o. Figure VI-7 shows on the upper trace a 32-MHz beat signal that vanishes on the lower trace when the stable laser is blocked.

Chirping of the TEA pulse can be expected for two reasons. The first is that the

refractive index of the CO_2 gas is proportional to χ', which goes as the product of the population inversion and the frequency separation of the oscillation from ν_o, and decreases rapidly during the formation of the pulse. The farther the TEA frequency is from the reference, the higher is the beat frequency; and the farther it is from ν_o, the more severe is the chirp. The change in the beat frequency can be either up or down, depending on the side of ν_o on which the TEA laser operates. This chirp is relatively rapid, and we refer to it as the "resonance effect." The second reason is that the refractive index of a gas at constant density is a function of temperature, and the kinetic temperature of the gas mixture increases ~50°C during the tail of the pulse which is 3 μs long. There are also dynamic changes in the vibrational temperature, especially of the nitrogen vibrational chain. This is a relatively slow change that would not be noticed during the time of the peak, but might be observed during the long tail. We refer to this as the "thermal effect."

The optical frequency change from the thermal effect will always be in the same direction, in contradistinction to that for the resonance effect. The change in the beat frequency for both effects can be in either direction.

A 10-MHz change in optical frequency can be caused by a change in refractive index of less than 1 in 10^6. This is the order of the change in χ'; the magnitude of the thermal effect has not been similarly estimated.

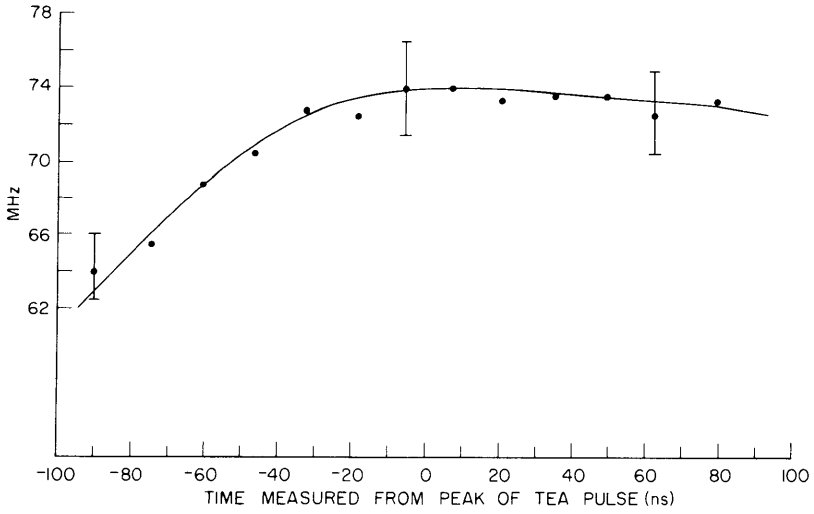

Fig. VI-8. Instantaneous beat frequency during the peak of a pulse.

Both effects have been observed and measured. In Fig. VI-6 the frequency rises from 46 MHz to 60 MHz during the rising edge and falls to 57 MHz at the half-power point. Figure VI-8 presents the dynamic frequency during the peak of another pulse; it shows a strikingly similar dependence on time during the peak. In other photographs,

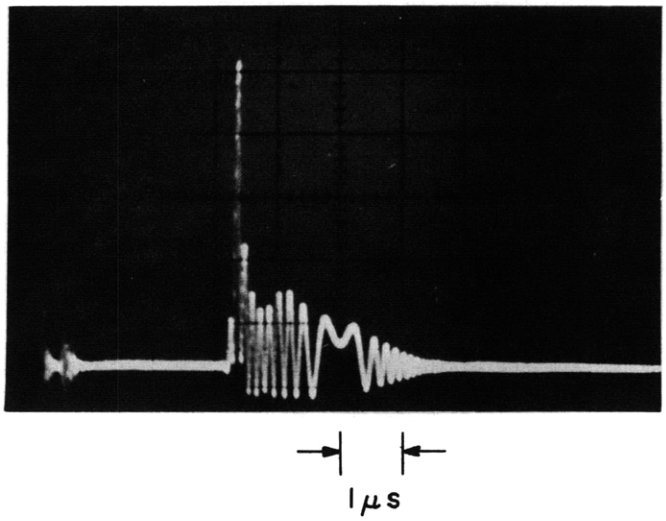

Fig. VI-9. Illustrating the thermal effect.

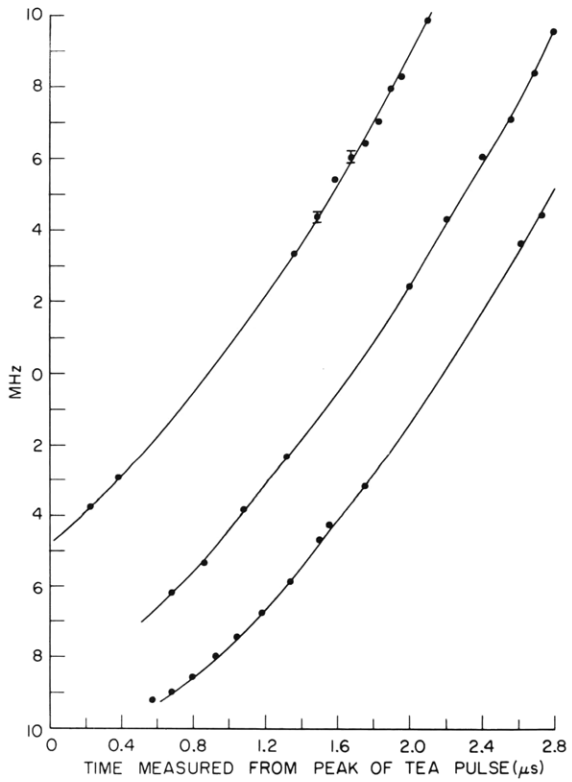

Fig. VI-10. Measurement of the thermal effect.

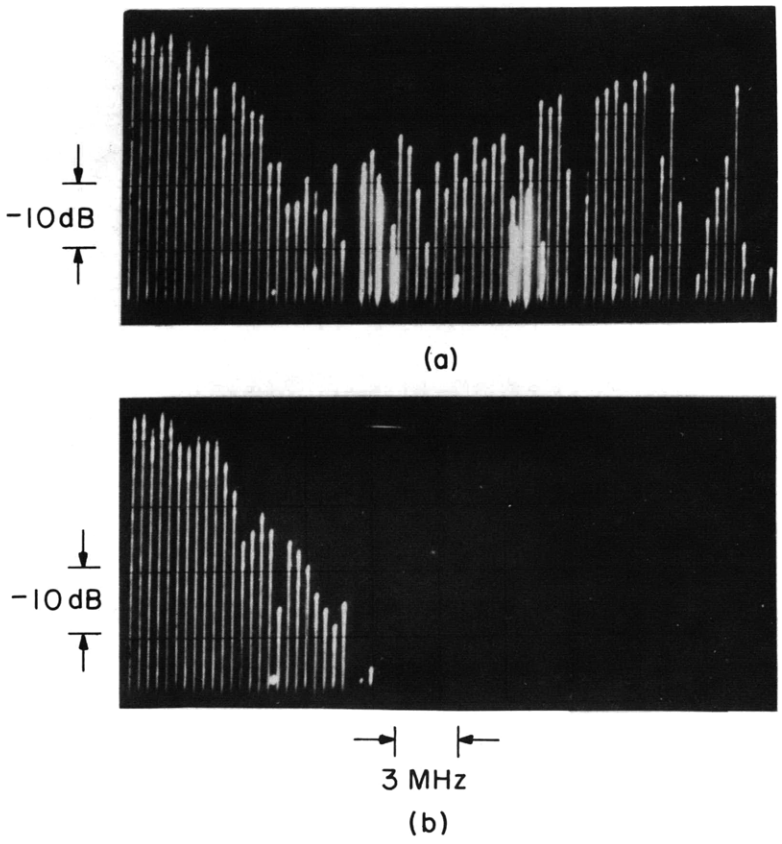

Fig. VI-11. Frequency spectra (a) with and (b) without the beat.

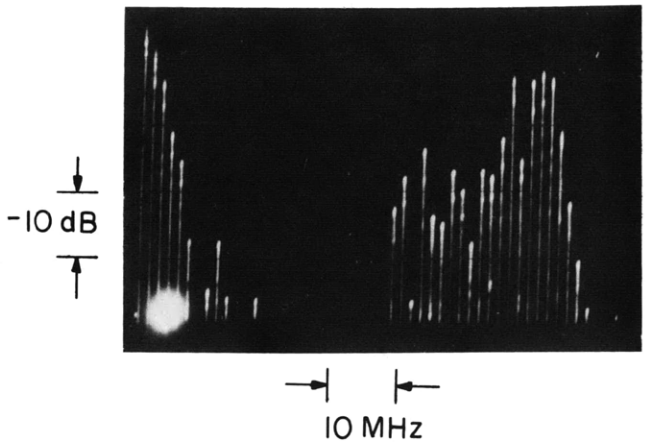

Fig. VI-12. Frequency spectrum showing different frequencies during the high peak and the long tail of the TEA pulse.

the change is in the opposite direction. In one case, a low-frequency beat (indicating oscillation near the reference frequency) shows no chirping during the formation of the pulse (indicating oscillation at ν_o, since there is no resonance effect).

To produce Fig. VI-9, the cavity length was adjusted so that the beat frequency passed through zero during the tail of the pulse. Figure VI-10 shows the thermal effect quantitatively. Plotted are the dynamic frequencies during the tails of three different pulses; the middle curve is for the pulse displayed in Fig. VI-9. The slope indicates the effect of the change in kinetic temperature of the gas and might vary with mixture ratios; it is reassuring that the curves are parallel.

Figure VI-11 does not show a conventional spectrum. The vertical lines indicate that the signal passed through a frequency "window" positioned at that frequency at the time of one pulse. In Fig. VI-11a the beat frequency during the peak is at the right. The chirping toward lower frequencies is of the size that would be predicted from the slope of the curves in Fig. VI-10. In Fig. VI-11b the stable laser was blocked. This is the envelope of the spectrum of the TEA pulse.

Figure VI-12 shows more clearly the difference in frequency during the peak and the tail. The spreading of the spectrum toward lower frequencies is due to chirping of the same magnitude as that observed in Fig. VI-11a. The resonant effect is not apparent because it happens so quickly. Figures VI-11 and VI-12 may be slightly distorted because of a slow thermal drift of the TEA frequency of ~4 MHz/min. The time for a full sweep of the spectrum analyzer is 35 seconds.

3. Conclusion

The frequency of TEA CO_2 laser radiation has been shown to be near line center and extremely stable from pulse to pulse. By reducing the partial pressure of N_2 in order to preclude the tail, and by operating near line center to minimize the resonance effect, it is possible to generate high-power, frequency-stable and nearly monochromatic pulses at a high repetition rate. These pulses can be tuned to many discrete wavelengths in the infrared by selecting different transitions of the CO_2 molecule and, possibly, other gases. If the resonance effect can be tolerated, then the source will be tunable throughout wide bands in the infrared.

W. A. Stiehl

References

1. A. J. Beaulieu, "Transversely Excited Atmospheric Pressure CO_2 Lasers," Appl. Phys. Letters 16, 504-505 (1970).
2. H. Nishihara and B. Kronast, "An Investigation of the Line Structure of a Helical TEA-CO_2-Laser," Opt. Commun. 5, 65-67 (1972).
3. A. Nurmikko, T. A. DeTemple, and S. E. Schwarz, "Single-Mode Operation and Mode Locking of High-Pressure CO_2 Lasers by Means of Saturable Absorbers," Appl. Phys. Letters 18, 130-132 (1971).
4. A. J. Beaulieu, "High Peak Power Gas Lasers," Proc. IEEE 59, 667-674 (1971).